analytical chemistry

Article

Cite This: Anal. Chem. 2020, 92, 1502−1510

pubs.acs.org/ac

Inhibitors in Commercially Available 2,2′-Azino-bis(3-ethylbenzothiazoline-6-sulfonate) Affect Enzymatic Assays

Yifei Zhang* and Henry Hess

Department of Biomedical Engineering, Columbia University, 351L Engineering Terrace, 1210 Amsterdam Avenue, New York, New York 10027, United States

Supporting Information

ABSTRACT: ABTS, 2,2′-azino-bis(3-ethylbenzothiazoline-6-sulfonate), is a common chromogenic substrate for peroxidase enzymes, which are widely used in biochemical research and diagnostic tests. We discovered that impurities in the commercially available ABTS significantly affect the results of peroxidase activity assays. We show that the impurities inhibit the activity of the peroxidases and the influence varies for different batches of ABTS from the same source. The inhibition of horseradish peroxidase (HRP) is uncompetitive for the substrate H_2O_2 while it is competitive for the substrate ABTS. By using high-resolution mass spectrometry, potential inhibitors were identified to be precursors or analogs of ABTS. The inhibitors are also capable of inhibiting the GOx-catalyzed reduction of the ABTS radical cation by glucose in anaerobic conditions. As the inhibition is found to be pH-dependent, diagnostic applications, such as ELISA tests based on the peroxidase-H_2O_2-ABTS system, should be carried out at pH 4.4 to minimize the inhibitory effect of potentially present impurities.

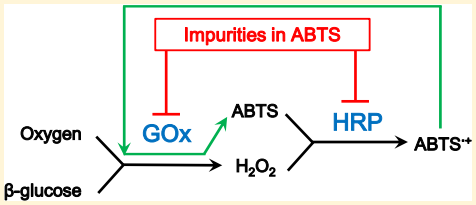

Enzymatic assays are the basis of a wide variety of clinical and point-of-care diagnostics for disease-related biomarkers ranging from small molecular metabolites (e.g., glucose and lactate) to biomacromolecules (e.g., specific enzymes and antibodies).[1−4] The assays are usually performed with ultralow concentrations of enzymes in a picomolar to nanomolar range in the presence of necessary substrates or coenzymes, which are usually commercially available. Given that the typical purity of common reagents is in the range of 95−99.9% and that the concentrations of substrates or coenzymes are usually 3−6 orders of magnitude higher than the enzymes of interest in assays, the number of impurity molecules in the reagents is comparable to the number of enzyme molecules and consequently large enough to significantly affect the assay results. Therefore, enzymatic assays could be more sensitive to the species and amounts of impurities in reagents than nonenzymatic ones, leading to variations in the results of diagnostic tests using different batches of reagents.

Horseradish peroxidase (HRP) is a monomeric metalloenzyme with a ferriporphyrin at the active center. Once activated by H_2O_2, it can react with various aromatic compounds such as phenols, anilines, and benzidines.[5,6] It is widely used as a reporter enzyme in diagnostic tests, immunochemical assays (ELISA, Western Blot, immunohistochemistry, etc.), and as a model enzyme in scientific research because of its ability to sense the level of hydrogen peroxide colorimetrically or fluorescently in the presence of chromogenic or fluorogenic substrates, respectively.[7−14] ABTS, 2,2′-azino-bis(3-ethylbenzothiazoline-6-sulfonic acid), is a common substrate for HRP, which is able to react with hydrogen peroxide to yield the blue/green colored radical cation, $ABTS^{\bullet+}$. It has been widely used as a chromogenic substrate for enzymatic assays[15] and enzyme-linked immunosorbent assays (ELISA),[16] an electron mediator for bioelectrocatalysis,[17] and as a reducing agent for antioxidant capacity assays in functional food analysis.[18]

In this study, we demonstrate that the activity of HRP is significantly affected by the quality of the chromogenic substrate, ABTS, and we describe the effect of the impurities on the activity of this widely used enzyme. The impurities in commercially available ABTS from Sigma-Aldrich, Inc., exhibit uncompetitive inhibition with respect to the first substrate H_2O_2 and exhibit competitive inhibition with respect to ABTS. Different batches of ABTS can cause the activity of HRP to vary severalfold. We suspected that the cause of the variable activity is the varying degree of contamination with ABTS analogs such as precursors and unsulfonated and partially sulfonated products formed during the chemical synthesis. These inhibitors can not only suppress the activity of HRP but also the activity of glucose oxidase as it catalyzes the reduction of the ABTS radical cation, $ABTS^{\bullet+}$, by glucose.[19] As ABTS is a common chromogenic substrate for enzyme-linked immunosorbent assays (ELISA), we evaluated the influence of the impurities on ELISA applications. Since the inhibition of HRP is undetectable at pH 4.4 and becomes stronger as pH increases, we suggest that the diagnostic assays need to be performed at pH 4.4 to achieve the highest sensitivity and reproducibility.

Received: October 17, 2019
Accepted: December 4, 2019
Published: December 4, 2019

DOI: 10.1021/acs.analchem.9b04751
Anal. Chem. 2020, 92, 1502−1510

EXPERIMENTAL SECTION

Materials. Two batches of ABTS, 2,2′-azino-bis(3-ethylbenzothiazoline-6-sulfonic acid) diammonium salt (product number A1888, lot number SLBV5859 and SLBZ8095), hydrogen peroxide (30%, product number 216763, lot number MKBV3835V), peroxidase from horseradish (essentially salt-free, P2088, lot number SLBN0615V), and HRP-conjugated goat antirabbit IgG (12-348, lot number 3277135) were purchased from Sigma-Aldrich Merck.

Enzymatic Assays. All of the enzymatic assays were carried out with an ultraviolet−visible spectrophotometer (Evolution 201, Thermo Scientific, USA). The concentration of HRP in aqueous solution was determined by its absorbance at 403 nm (ε_{403nm} = 1.02 × 10^5 M^{-1} cm^{-1}).[20] The activity of HRP was measured at various concentrations of H_2O_2 (1−500 μM) and ABTS (0.1−4 mM) in 1×PBS buffer (pH 7.4) containing 1.0 nM HRP by following spectrophotometrically the changes in absorbance at 415 nm for 1 min using the spectrophotometer ($\varepsilon_{415\ nm}$ = 3.6 × 10^4 M^{-1} cm^{-1}).[21]

The GOx-HRP cascade reaction was carried out in a quartz cuvette with a light-path of 2 mm, and the reaction was monitored at 635 nm with the spectrophotometer. The cuvette was sealed immediately with a piece of plastic paraffin film after it was filled to the top with 1.15 mL of assay solution (e.g., 100 nM GOx, 200 nM HRP, 100 mM glucose, and 2 mM ABTS).

Mass Spectroscopy. High-resolution mass spectrometry was performed on a Waters Xevo G2-XS QToF mass spectrometer equipped with a H-Class Plus UPLC inlet, a Z-Spray ion source with LockSpray, and an ESI probe. The samples were dissolved in ddH_2O at a concentration of 1.0 mM.

Colorimetric Assay of IgG-HRP Conjugate. The colorimetric assays of IgG-HRP conjugate were carried out in 100 mM citric-phosphate buffers at pHs of 4.0, 4.2, 4.4, 4.8, 5.2, 5.8, 6.2, and 7.0. In a typical run, 100 μL of HRP-conjugated goat antirabbit IgG solution with concentrations ranging from 0 to 100 ng/mL was added in each well of a 96-well ELISA plate. Then, the reaction was initiated by adding 100 μL of substrate solution containing 2 mM ABTS and 1 mM H_2O_2. After incubation at room temperature for 30 min, the reaction was stopped by adding 10 μL of stop solution (10% SDS in 50% dimethylformamide−water solution). The absorbance was measured at 415 nm on a Tecan Infinite 200 PRO microplate reader.

RESULTS AND DISCUSSION

Different Batches of ABTS Exhibit Varied Inhibition toward HRP. The mechanism of HRP-catalyzed oxidation of ABTS by H_2O_2 has been well-documented decades ago.[15,22] Initially, HRP rapidly reacts with equimolar H_2O_2 to form an HRP−H_2O_2 complex (k_1 > 10^7 M^{-1} s^{-1}),[23] followed by heterolytic cleavage of the oxygen−oxygen bond to give an oxyferryl porphyrin π-cation radical intermediate, Compound I, transferring two electrons from the ferric enzyme to H_2O_2. The reducing agent ABTS can then reduce compound I to compound II containing an oxyferryl heme and afterward return it to its resting state via two successive single electron transfer steps. Each step involves the formation of the corresponding enzyme−ABTS complex and the release of one molecule of $ABTS^{\bullet+}$ (Scheme 1). The release of $ABTS^{\bullet+}$ from the compound II−ABTS complex is considered to be the rate-limiting step in the catalytic cycle. Although the mechanism would be more complicated if the reducing agent is limited,[24,25] in most cases and particularly in diagnostic applications, the concentration of ABTS is much greater than the concentration of H_2O_2. Therefore, the reaction mechanism as well as the reaction stoichiometry comply with Scheme 1 in this study.

Scheme 1. Catalytic Cycle of the HRP-Catalyzed Reaction of H_2O_2 with ABTS

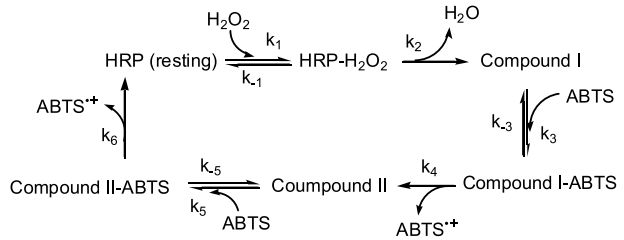

The rate equation derived from Scheme 1 obeys the well-known Ping-Pong Bi−Bi kinetics[26,27]

$$v = \frac{d[ABTS^{\bullet+}]}{dt} = 2k_6[\text{compound II—ABTS}] = \frac{2k_{cat}E_T}{\frac{K_{m,H_2O_2}}{[H_2O_2]} + \frac{K_{m,ABTS}}{[ABTS]} + 1} \quad (1)$$

where

$$K_{m,H_2O_2} = \frac{k_{cat}(k_{-1} + k_2)}{k_1k_2}$$

$$K_{m,ABTS} = k_{cat}\left(\frac{k_{-3} + k_4}{k_3k_4} + \frac{k_{-5} + k_6}{k_5k_6}\right)$$

$$k_{cat} = \frac{1}{\frac{1}{k_2} + \frac{1}{k_4} + \frac{1}{k_6}}$$

and E_T is the total concentration of the enzyme HRP. When the activity assay of HRP is carried out at a fixed concentration of ABTS, the Ping-Pong Bi−Bi rate equation can be written in the form of the Michaelis−Menten rectangular hyperbola

$$v = \frac{2E_Tk_{cat,app}[H_2O_2]}{K_{m,app} + [H_2O_2]} \quad (2)$$

where

$$k_{cat,app} = \frac{k_{cat}}{K_{m,ABTS}/[ABTS] + 1}$$

and

$$K_{m,app} = \frac{K_{m,H_2O_2}}{K_{m,ABTS}/[ABTS] + 1}$$

We obtained two batches of ABTS from Sigma-Aldrich under the same product number, A1888, but with two different lot numbers, SLBV5859 (abbreviated as ABTS-V) and SLBZ8095 (abbreviated as ABTS-Z). As stated in the product specifications, the purity by HPLC of these products is higher than 98%. We determined the $ABTS^{\bullet+}$ production rates of the same HRP by using these two batches of ABTS. Surprisingly, the measured activity using ABTS-Z appears 3-fold higher than using ABTS-V, indicating that at least the activity of HRP was

DOI: 10.1021/acs.analchem.9b04751
Anal. Chem. 2020, 92, 1502−1510

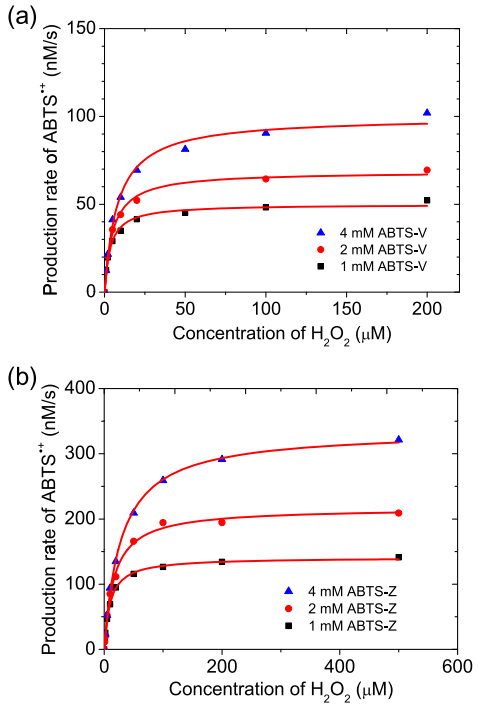

Figure 1. Activity assays of 1.0 nM HRP with two batches (V,Z) of ABTS: (a) ABTS-V and (b) ABTS-Z.

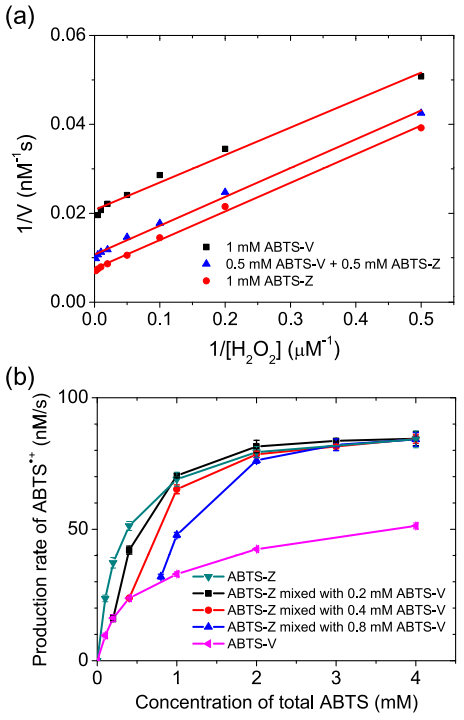

Figure 2. (a) Lineweaver–Burk plots of HRP activity with respect to H_2O_2 in the presence of 1 mM ABTS-V, 0.5 mM ABTS-V + 0.5 mM ABTS-Z or 1 mM ABTS-Z. (b) The production rates of $ABTS^{\bullet+}$ as a function of concentration of mixed ABTS in 10 μM H_2O_2. All assays were carried out in triplicate with 1 nM HRP in PBS buffer at pH 7.4.

inhibited when using ABTS-V as the substrate (Figure 1). The apparent kinetic parameters were determined by nonlinear fitting with the Michaelis–Menten function and are listed in Table 1. The apparent turnover number, $k_{cat,app}$ (with respect to the conversion of H_2O_2) increases in a higher concentration of ABTS-V or ABTS-Z, and the apparent $K_{m,app}$ for H_2O_2 increases proportionally. At a given concentration of ABTS, the $k_{cat,app}/K_{m,app}$ with respect to H_2O_2 remains similar for both ABTS batches.

We also measured the activity of HRP-catalyzed ABTS oxidation using a mixture of ABTS-V and ABTS-Z and found that the apparent activities of HRP are always in between the activities with ABTS-V and with ABTS-Z. The parallel lines in the Lineweaver–Burk plots prove that the inhibition was uncompetitive with respect to H_2O_2 (Figure 2a). By increasing the content of ABTS-Z in the mixture, the production rate of $ABTS^{\bullet+}$ approaches the activity measured with ABTS-Z only (Figure 2b). This indicates that the inhibition effect is competitive with respect to ABTS, therefore the inhibitors are probably analogs of ABTS.

Probable Inhibitors Are Precursors from the Chemical Synthesis of ABTS. We determined the ultraviolet–visible spectra of 10.0 μM ABTS-V and 10.0 μM ABTS-Z dissolved in PBS buffer and found that the spectra are identical to those in previous reports (Figure S1).[19,28] The absence of new absorption peaks indicates that the impurities in ABTS-V may have similar chromophores compared to pure ABTS. The absorption peaks of ABTS-Z at 224 and 340 nm are 4% higher than those of ABTS-V, suggesting that the ABTS-V may contain a bit more contaminations, such as water or salts, which make a negligible contribution to the absorbance in the range of 200–800 nm. Obviously, such small differences in ABTS concentration cannot cause the large variation in the activity assays.

We employed high-resolution mass spectrometry to identify the suspected inhibitors in ABTS-V and ABTS-Z. As shown in Figure 3, ABTS-V contains much more impurities than ABTS-Z. The impurities most likely get into the product during chemical synthesis. The key step in preparing ABTS is the synthesis of 2,2′-azino-bis(3-ethylbenzothiazoline) (**1**), which is subsequently sulfonated by H_2SO_4 and neutralized with ammonia to afford ABTS diammonium salt (**3**) (Scheme 2a). Three feasible synthetic routes are illustrated in Scheme 2b–d. Chen et al.[29] proposed that **1** can be synthesized from the coupling of 3-ethyl-2-iminobenzothiazoline bromide (**4**) with 3-ethyl-2-benzothiazolinone hydrazone (**5**) (Scheme 2b).

Table 1. Kinetic Parameters of HRP Reacting with Different Batches of ABTS

	1 mM ABTS		2 mM ABTS		4 mM ABTS	
	ABTS-V	ABTS-Z	ABTS-V	ABTS-Z	ABTS-V	ABTS-Z
$k_{cat,app}$ (s^{-1})	25 ± 1	70 ± 1	34 ± 1	108 ± 2	50 ± 1	168 ± 2
$K_{m,app}$ (μM)	3.5 ± 0.4	10.0 ± 0.4	5.1 ± 0.5	16.5 ± 1.1	8.0 ± 0.8	28.7 ± 1.1
$k_{cat,app}/K_{m,app}$ (μM^{-1} s^{-1})	7.1 ± 1.1	7.0 ± 0.4	6.7 ± 0.9	6.5 ± 0.6	6.3 ± 0.8	5.9 ± 0.3
$k_{cat\text{-}Z,app}/k_{cat\text{-}V,app}$	2.8 ± 0.2		3.1 ± 0.1		3.5 ± 0.1	
$K_{m\text{-}Z,app}/K_{m\text{-}V,app}$	2.9 ± 0.4		3.2 ± 0.5		3.6 ± 0.5	

DOI: 10.1021/acs.analchem.9b04751
Anal. Chem. 2020, 92, 1502–1510

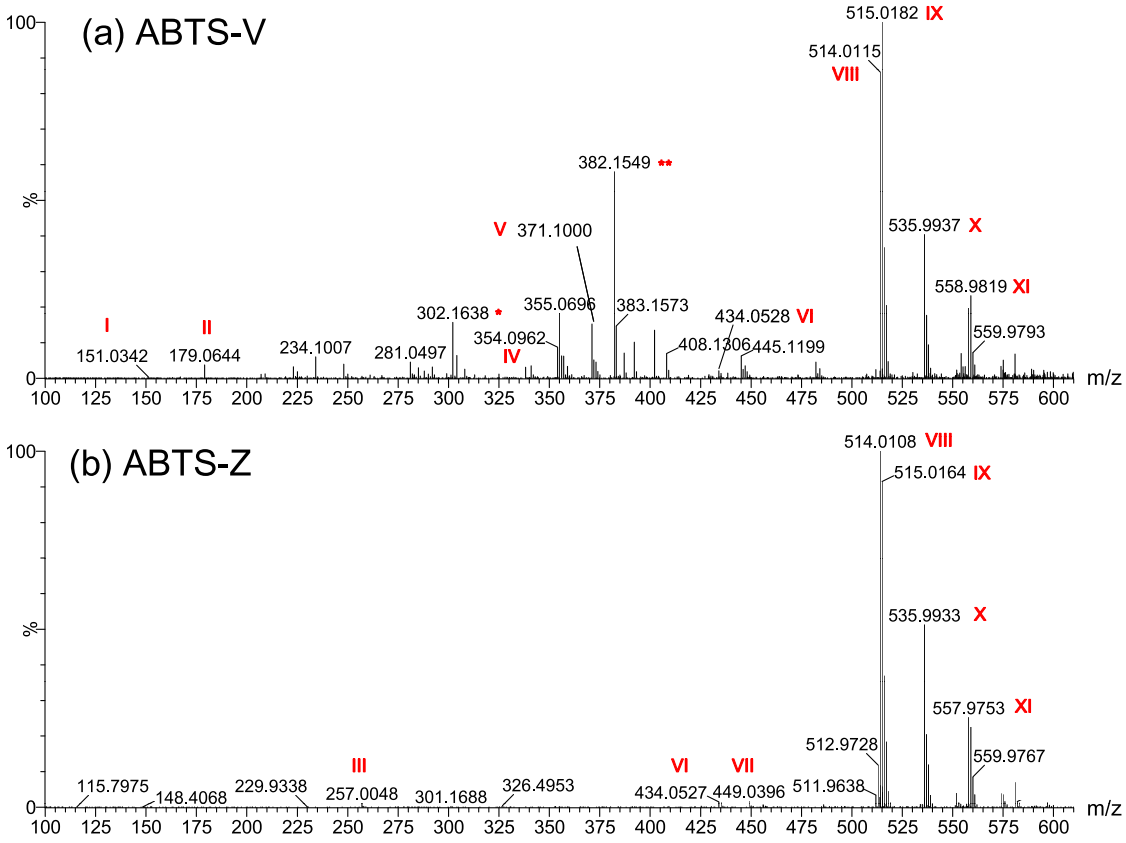

Figure 3. Mass spectra of (a) ABTS-V and (b) ABTS-Z.

Scheme 2. Possible Synthetic Routes to ABTS Diammonium Salt

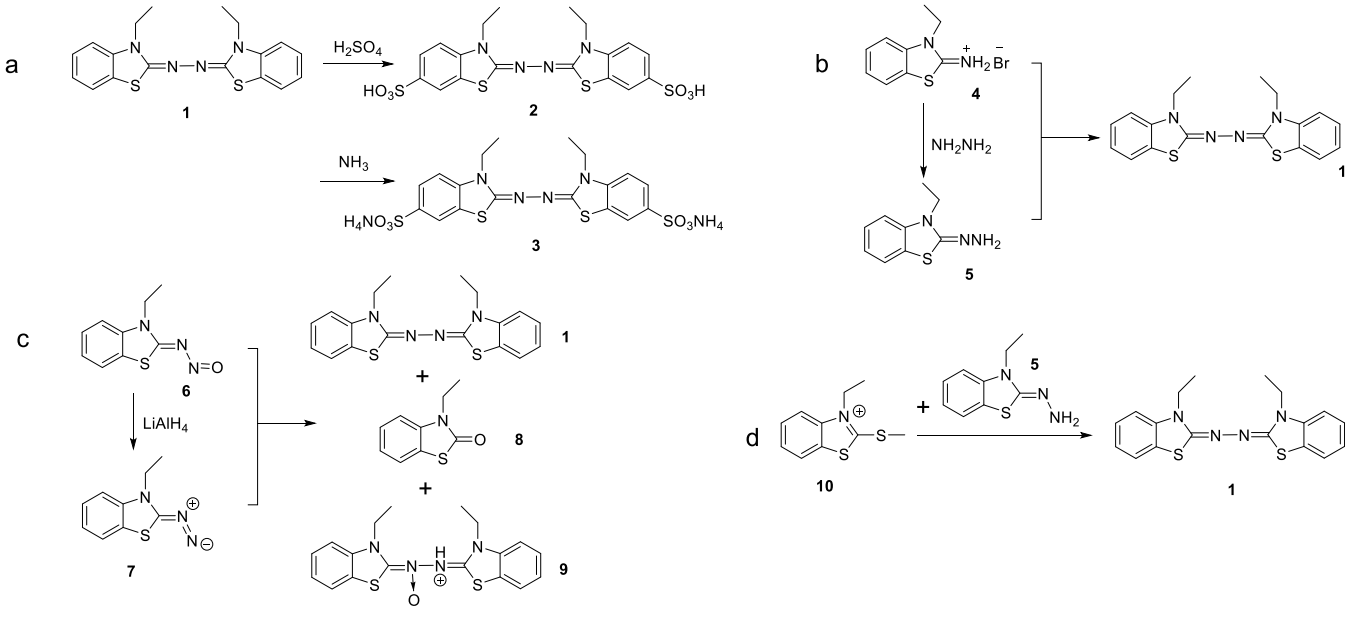

Akiba et al.[30] showed another feasible approach starting from the reduction of 3-ethyl-2-nitrosoimino-2,3-dihydrobenzothiazole (**6**) by lithium aluminum hydride ($LiAlH_4$) and followed by the reaction of **6** with the produced 2-diazo-3-ethyl-2,3-dihydrobenzothiazole (**7**). Byproducts, such as the 3-ethyl-2(3*H*)-benzothiazolone (**8**) and the azine *N*-monoxide (**9**), will form during the synthesis (Scheme 2c). Fei et al.[31] reported that the reaction of 2-methylthio-3-ethyl-benzothiazolium salt with **5** will yield the precursor of ABTS (Scheme 2d).

We identified a few impurities in ABTS-V according to the high-resolution mass spectra (Table 2). The compounds, such as reactant **4**, the ABTS precursor **1**, and its monosulfonated form, azine *N*-monoxide **9**, can be found. The existence of these compounds implies that the commercial ABTS was synthesized via the routes shown in Scheme 2b or 2c rather

DOI: 10.1021/acs.analchem.9b04751
Anal. Chem. 2020, 92, 1502−1510

Table 2. Compounds Detected in Mass Spectra of ABTS-V and ABTS-Z

Marks in Figure 3	Structure of Ionized Compounds	Detected m/z	Theoretical m/z (monoisotopic)	Compound No.
I	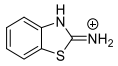	151.0342	151.0324	Compound **4** without ethyl group
II	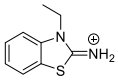	179.0644	179.0637	Compound **4**
III	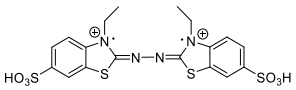	257.0048	257.0049	Compound **2**
IV	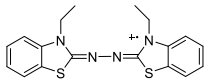	354.0962	354.0967	Compound **1**
V	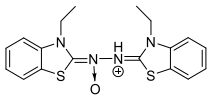	371.1000	371.0995	Compound **9**
VI	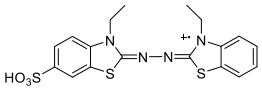	434.0528	434.0536	Monosulfonated **1**
VII	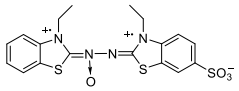	449.0396	449.0406	Monosulfonated **9**
VIII	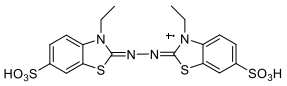	514.0115	514.0104	Compound **2**
IX	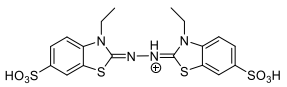	515.0182	515.0182	Compound **2**
X	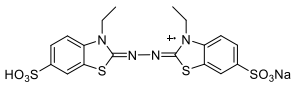	535.9937	535.9923	Compound **2**
XI	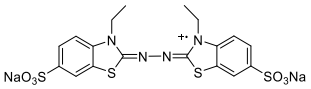	557.9749	557.9743	Compound **2**

than the route shown in Scheme 2d. The most abundant impurity with molecular weight of 382.1549 remains unknown. However, it is obviously a monosulfonated form of another unknown compound with molecular weight of 302.1638 (ΔM_w = 79.9911), indicating both of them are aromatic compounds which can potentially act as competitive inhibitors for HRP.[32] The monosulfonated **1** and azine *N*-monoxide **9** are also found in ABTS-Z (Figure 3b, VI and VII).

It has been well-documented that the activity of HRP itself is pH dependent with a pH optimum around pH 4−6.[33,34] Interestingly, the inhibition by the impurities in ABTS is also highly pH dependent. The activity of HRP reacting with ABTS-Z was approximately 3-fold higher than that with ABTS-V if the solution pH is higher than 7. Decreasing the solution pH can gradually reduce and finally completely eliminate the inhibitory effect. This suggests that the protonated inhibitors do not inhibit the activity of HRP. Given that the active site residues His42 and Arg38 of HRP are positively charged at acidic pH,[35] we presume that the protonated inhibitors (such as compound **1** and its monosulfonated form, as well as compound **4** and **9**) are also positively charged so that they are blocked from the active site.

We have to point out that ABTS-Z cannot be considered an ABTS standard without inhibition toward HRP. We used to have a third batch of ABTS (the same product number, A1888) with a lot number of SLB**P**8174V (abbreviated as ABTS-P) in our previous research, which exhibited an $ABTS^{\bullet+}$ production rate of 540 nM/s by the same batch of HRP (1.0 nM) at pH 7.4 (Figure 4, green triangle),[19] approximately 2.7-fold higher than the activity with ABTS-Z. Thus, we conclude that both ABTS-Z and ABTS-V contain competitive inhibitors for the intermediate states of HRP. However, the activity of HRP is identical at pH 4.4 for all batches of ABTS, indicating that the inhibition is strongly pH dependent (Figure 4). Pure ABTS could have at least 8-fold higher reactivity with HRP compared with the bad batch of ABTS when the assays are carried out at neutral pH conditions, which are used in a number of investigations.[36−40]

The pH-dependent inhibition toward HRP by the impurities in ABTS has implications for the measured activity enhancements of the GOx-HRP cascade immobilized on DNA nanostructures.[11,36,41,42] We have studied this system in detail and have concluded that a permanent enhancement in cascade activity has to originate from the increased activity of the rate-limiting enzyme rather than the hypothesized substrate

DOI: 10.1021/acs.analchem.9b04751
Anal. Chem. 2020, 92, 1502−1510

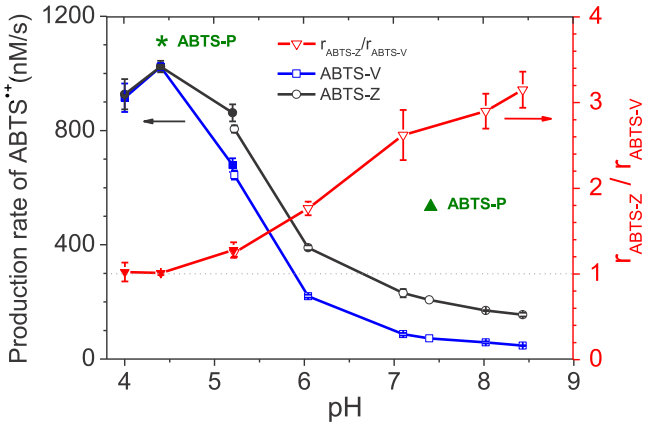

Figure 4. pH-dependent inhibitory effect of the impurities in ABTS. The reaction rates were measured in triplicate with 1 nM HRP, 2 mM ABTS-V or ABTS-Z, and 500 μM H_2O_2 in varying buffers: 100 mM citrate buffer at pH 4.0, pH 4.4, and pH 5.2 (solid symbols); 50 mM phosphate buffers at pH 5.2, 6.1, 7.1, 8.0, 8.4 (open symbols); and 10 mM PBS buffer at pH 7.4, respectively. The reaction rates of HRP with ABTS-P are marked with a green star (pH 4.4) and a green triangle (pH 7.4).

channeling.[34,43−46] We suggested that a possible reason for the activity enhancement of enzymes (e.g., HRP) on DNA nanostructures is the relatively acidic microenvironment provided by the highly negatively charged DNA surface.[34] Here, we showed that the inhibition effect of a contaminated substrate toward HRP can be reduced significantly by lowering the solution pH. Therefore, a shift of the pH in the environment of the HRP molecule affects its activity by two distinct mechanisms: it increases its intrinsic activity and it reduces the inhibitory effect of the substrate impurities. Thus, the magnitude of the observed effect may appear to be highly variable if the experiments do not control for the batch of ABTS used. The interactions between the ABTS impurities and the DNA nanostructure further complicate the picture and deserve further examination.[11,14,36,37,47,48]

The inhibitory mechanism is shown in Scheme 3. Under the steady-state approximation and assuming that the inhibitors can bind compounds I and II with different affinities, one can derive the rate equation describing the ping-pong kinetics with competitive inhibition

$$v = 2E_T \Bigg/ \Bigg\{ \frac{k_{-1}+k_2}{k_1 k_2 [H_2O_2]} + \Bigg[\frac{k_4+k_{-3}}{k_3 k_4} + \frac{k_6+k_{-5}}{k_5 k_6} + \frac{(k_4+k_{-3})k_{1i}[\mathrm{Inh}]}{k_3 k_4 k_{-1i}} + \frac{(k_6+k_{-5})k_{2i}[\mathrm{Inh}]}{k_5 k_6 k_{-2i}} \Bigg] \frac{1}{[\mathrm{ABTS}]} + \left(\frac{1}{k_2} + \frac{1}{k_4} + \frac{1}{k_6} \right) \Bigg\} \quad (3)$$

$$v = 2k_{cat}E_T \Bigg/ \Bigg\{ \frac{K_{m,H_2O_2}}{[H_2O_2]} + \Bigg[K_{m,ABTS} + \frac{(k_4+k_{-3})k_{1i}k_{cat}[\mathrm{Inh}]}{k_3 k_4 k_{-1i}} + \frac{(k_6+k_{-5})k_{2i}k_{cat}[\mathrm{Inh}]}{k_5 k_6 k_{-2i}} \Bigg] \frac{1}{[\mathrm{ABTS}]} + 1 \Bigg\} \quad (4)$$

We can define an inhibition constant K_i, which is an indication of the overall inhibitory effect of the inhibitors in a certain batch of ABTS

$$\frac{1}{K_i} = \frac{(k_4+k_{-3})k_{1i}k_{cat}}{k_3 k_4 k_{-1i}} + \frac{(k_6+k_{-5})k_{2i}k_{cat}}{k_5 k_6 k_{-2i}} \quad (5)$$

and obtain

$$v = \frac{2k_{cat}E_T}{\frac{K_{m,H_2O_2}}{[H_2O_2]} + \frac{K_{m,ABTS}}{[\mathrm{ABTS}]} + \frac{[\mathrm{Inh}]}{K_i[\mathrm{ABTS}]} + 1} \quad (6)$$

It is a very approximate description for the HRP-H_2O_2-ABTS reaction because the different batches of ABTS likely contain variable amounts of the different inhibitors and because the reaction pathways can be more complicated when the concentration of H_2O_2 is greater than that of ABTS.[25,49,50] Nevertheless, it clearly shows that for this mechanism the ratio of k_{cat} to K_{m,H_2O_2} is unaffected by the inhibitor concentration and that the inhibition is only competitive with ABTS.

Impurities Inhibit the GOx-Catalyzed ABTS$^{\bullet+}$ Reduction by Glucose. The HRP-ABTS system is commonly used for colorimetric enzymatic assays of flavin-dependent oxidases that utilize oxygen as an electron acceptor to produce H_2O_2. The glucose oxidase (GOx)-HRP cascade is the most widely studied enzyme pair owing to its potential clinical applications and its scientific value as a classic model system.[34,51,52] We discovered very recently that—in addition to serving as substrate for the well-known oxidase-peroxidase cascade reactions—ABTS$^{\bullet+}$ can act as a competitive substrate to oxygen for the oxidation of glucose, so that GOx can reduce ABTS$^{\bullet+}$ back to ABTS once oxygen levels are depleted.[19] With this reaction, we demonstrated the generation of multiple pulse

Scheme 3. Inhibitory Mechanism by Impurities

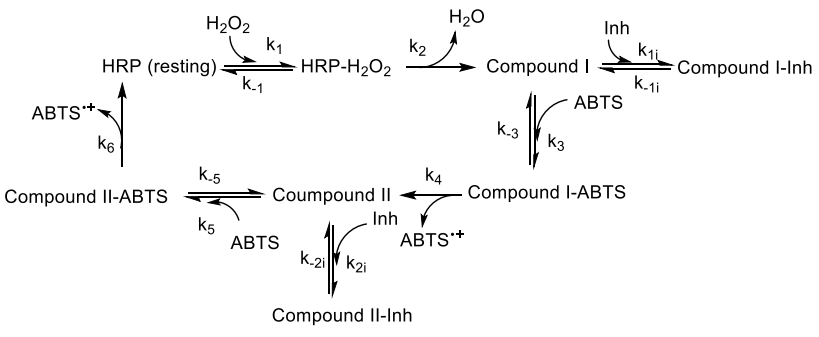

DOI: 10.1021/acs.analchem.9b04751
Anal. Chem. 2020, 92, 1502−1510

responses in a sealed cuvette and visualized the interfacial enzymatic reaction-driven Rayleigh–Bénard convection in real time.[19]

We tested if the impurities in ABTS also affect the activity of GOx utilizing $ABTS^{\bullet+}$ using the same experimental procedure described in ref 19. Interestingly, the impurities in ABTS not only inhibit the activity of HRP, but also significantly suppress the GOx-catalyzed reduction of $ABTS^{\bullet+}$. Figure 5a shows that

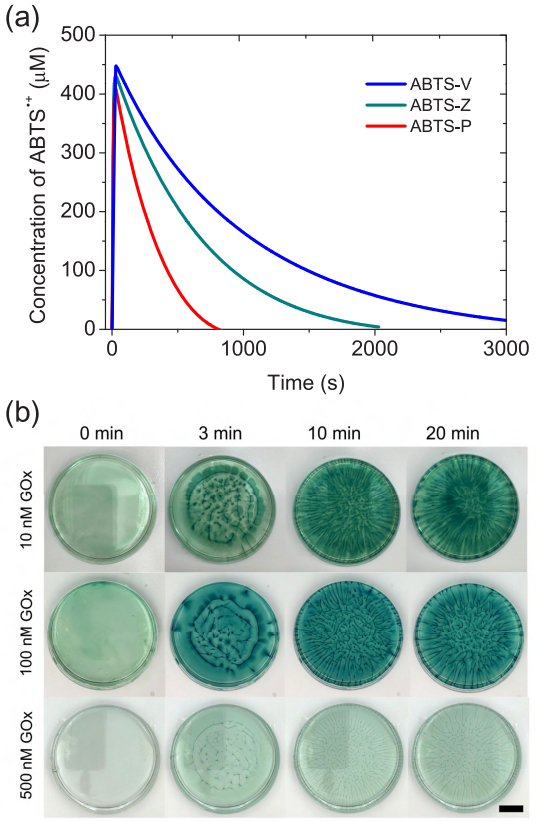

Figure 5. (a) GOx is inhibited by the impurities in different batches of ABTS as it catalyzes the conversion of $ABTS^{\bullet+}$ back to ABTS. The initial solutions contain 100 nM GOx, 200 nM HRP, 100 mM glucose, and 2 mM ABTS. (b) The activity of GOx, here modulated by changing the GOx concentration from 10 nM to 500 nM, affects the pattern formation in a solution in Petri dish with GOx and 200 nM HRP, 100 mM glucose, 1 mM ABTS-V in 30 mL of PBS buffer. Scale bar: 2 cm.

the reduction rates of $ABTS^{\bullet+}$ in the GOx-HRP system are ABTS batch-dependent. ABTS-Z, which shows higher peroxidase activity, gives also a higher reduction rate of $ABTS^{\bullet+}$ compared with ABTS-V (with a first order decay constant $k_{red,Z}$ of 1.6×10^{-3} s^{-1} for ABTS-Z versus $k_{red,V}$ of 1.0×10^{-3} for ABTS-V). ABTS-P, the batch with the least inhibition of HRP, shows an even higher reduction rate ($k_{red,p} = 3.3 \times 10^{-3}$ s^{-1}). This could be attributed to the competitive blocking of $ABTS^{\bullet+}$ by ABTS analogs from the active site of GOx. It is worth noting that the existence of the impurities does not affect the activity assay of glucose oxidase if an excess of HRP is applied (Figure S2). However, the different reduction rate of $ABTS^{\bullet+}$ influences the development of visible patterns in Rayleigh–Bénard convection. The visibility of convective patterns requires a proper contrast relying on a dynamic balance between the formation of colored $ABTS^{\bullet+}$ at the air–water interface and its reduction in the bulk solution. If the reduction of $ABTS^{\bullet+}$ is slower, the produced $ABTS^{\bullet+}$ cannot be rapidly reduced to the colorless ABTS as it is transported from the surface to the bulk solution, thus yielding a solution which is too dark green and has blurry patterns. To observe clear patterns, the production and reduction rates of $ABTS^{\bullet+}$ need to be balanced by adjusting the ratio of GOx and HRP. For example, increasing the concentration of GOx can facilitate the reduction of $ABTS^{\bullet+}$ and, therefore, optimize the appearance of the patterns (Figure 5b).

Performing ELISA Tests at Acidic pH Can Circumvent the Inhibition. ELISA tests typically use HRP as enzyme and *o*-phenylenediamine (OPD), 3,3′,5,5′-tetramethylbenzidine (TMB), and ABTS as substrates.[53] Because of the carcinogenicity of OPD, it is not recommended in most applications. Although ABTS had been found to be weakly mutagenic in an early study,[54] a later investigation suggested that the mutagenic activity originated from impurities in ABTS and varied in different batches.[55] Hence, to our knowledge, neither pure TMB nor pure ABTS are considered as carcinogenic or mutagenic substrates.[56,57] However, TMB is basically insoluble in water. Cosolvents, such as DMSO, DMF, or ethanol are necessary for dissolving TMB in assay buffers. For example, in PBS buffer mixed with 0.3% DMSO only 30 μg/mL TMB can be dissolved (https://www.caymanchem.com/pdfs/70450.pdf). This significantly narrows the dynamic range of ELISA tests (upper and lower concentrations of the analytes that can be accurately assayed) when using TMB as a substrate. In comparison, ABTS has a wider dynamic range[58] thanks to its roughly thousand-fold higher solubility (up to 50 mg/mL) in aqueous solutions (see the Product Information provided by Sigma-Aldrich, Inc.).

The pH conditions for the color development of ABTS-based ELISA tests vary from pH 4.0 to 7.0 in different reports.[59−70] Reagent companies also provide different suggestions for the assay pHs (e.g., Southern Biotech, pH 4.0; Sigma-Aldrich, pH 5.0; Kirkegaard & Perry Laboratories of SeraCare, pH 5−7). Considering the pH-activity profile of HRP and the potential inhibition, the assay pH has to be optimized to obtain the highest sensitivity and the lowest detection limit. Figure 6 shows the detection of HRP-labeled goat antirabbit IgG with ABTS-V and ABTS-Z at various pH conditions. The highest responses are found at pH 4.4 and pH 4.8, and dramatically decrease if the assay pH is lower than 4.2 and higher than 5.2. In agreement with Figure 4, the inhibition is eliminated at pH 4.4 and becomes more significant as the pH increases. The dramatic decrease in response and low sensitivity at pH 4.0 may be attributed to the thermal instability of HRP at acidic pH ranges.[71,72] Therefore, the optimization of ELISA performance is a compromise between the pH-activity profile, pH-dependent stability, and potentially present pH-dependent inhibition. As indicated in Figure 6, we suggest that the optimum pH for HRP/ABTS based ELISA tests is 4.4, where the detection limit is found to be 0.2 ng/mL IgG-HRP conjugate, ten times lower than the reference value given by Thermo Fisher Scientific (TR0033.4, Guide to enzyme substrates for ELISA).

CONCLUSION

Here, we investigate in detail the inhibitory effects of impurities in commercially available ABTS on the peroxidase activity of HRP and the reductive activity of GOx for $ABTS^{\bullet+}$. Surprisingly, different batches of ABTS products with the same

DOI: 10.1021/acs.analchem.9b04751
Anal. Chem. 2020, 92, 1502−1510

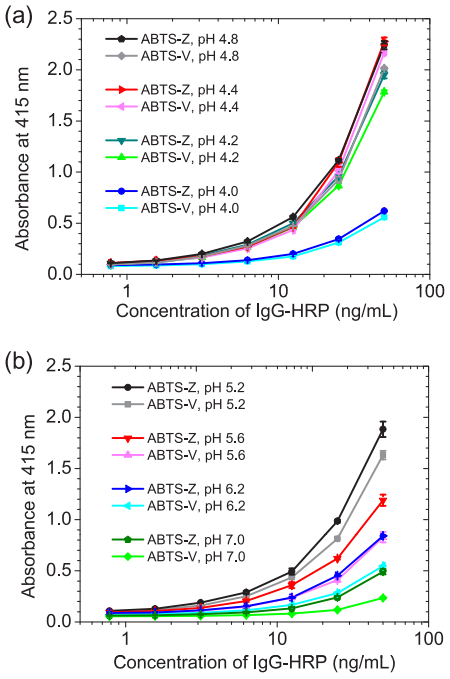

Figure 6. Chromogenic detection of IgG-HRP conjugate in citrate-phosphate buffer at various pH conditions. All assays were carried out in triplicate.

catalog numbers from Sigma-Aldrich can cause several-fold variations in the HRP activity assay due to the varied inhibition. We identify some impurities in the commercial ABTS by using high-resolution mass spectroscopy and suggest that the inhibitors are most likely precursors of ABTS introduced during the chemical synthesis of ABTS. Such inhibition is competitive for ABTS but uncompetitive for H_2O_2 and is highly pH-dependent. The batch-dependent inhibition affects the visualization of convective patterns in solutions of GOx-HRP system because the impurities also inhibit the conversion of $ABTS^{\bullet+}$ to ABTS by GOx, requiring a tuning of the concentrations of enzymes. For ELISA tests using ABTS as a chromogen, a substrate solution with pH 4.4 is recommended to avoid the potential inhibition by impurities in ABTS.

The quality control of chemical reagents is crucial for the reproducibility and replicability of scientific research. Although the quality of chemical reagents is often specified by their purity, standard levels of purity may not be sufficient for biochemical applications, especially assays based on specific interactions with biomacromolecules. The existence of impurities that formed during the synthesis of target chemicals, even in small amounts, can significantly affect biochemical assays due to the chemical similarity between precursors and target chemicals. Therefore, we suggest that a specification describing the biological activity of these reagents toward targeted proteins or enzymes is urgently needed.

■ ASSOCIATED CONTENT

Supporting Information

The Supporting Information is available free of charge at https://pubs.acs.org/doi/10.1021/acs.analchem.9b04751.

UV−vis spectra of ABTS-V and ABTS-Z; the activity assay of glucose oxidase in the presence of ABTS-Z or ABTS-V; and the kinetic parameters of HRP in phosphate buffers at pH 5.2, 6.1, and 7.1 (PDF)

■ AUTHOR INFORMATION

Corresponding Author

*E-mail: yz2930@columbia.edu.

ORCID

Yifei Zhang: 0000-0002-0014-611X

Henry Hess: 0000-0002-5617-606X

Author Contributions

Y.Z. and H.H. conceived and designed the research. Y.Z. performed the experiments. All authors discussed the results and contributed to editing the manuscript.

Notes

The authors declare no competing financial interest.

■ ACKNOWLEDGMENTS

We thank Dr. Brandon Fowler from the Mass Spectrometry Core Facility of the Department of Chemistry at Columbia for his help with the mass spectrometry. This work was supported by the NSF under Award Number NSF-ENG 1844149.

■ REFERENCES

(1) Zhang, J.; Chai, X.; He, X.; Kim, H. J.; Yoon, J.; Tian, H. *Chem. Soc. Rev.* **2019**, *48*, 683−722.

(2) Wanders, R. J. A.; Poorthuis, B. J. H. M.; Rodenburg, R. J. T. Enzymes, Metabolic Pathways, Flux Control Analysis, and the Enzymology of Specific Groups of Inherited Metabolic Diseases. In *Inherited Metabolic Diseases*; Hoffmann, G. F., Zschocke, J., Nyhan, W. L., Eds.; Springer: Berlin, 2010.

(3) Raja, M. M. M.; Raja, A.; Imran, M. M.; Santha, A. M. I.; Devasena, K. *Biotechnology* **2011**, *10*, 51−59.

(4) Schleicher, E. *Anal. Bioanal. Chem.* **2006**, *384*, 124−131.

(5) Nicell, J. A.; Bewtra, J. K.; Biswas, N.; St. Pierre, C. C.; Taylor, K. E. *Can. J. Civ. Eng.* **1993**, *20*, 725−735.

(6) Henriksen, A.; Schuller, D. J.; Meno, K.; Welinder, K. G.; Smith, A. T.; Gajhede, M. *Biochemistry* **1998**, *37*, 8054−8060.

(7) Guida, V.; Cantarella, M.; Chambery, A.; Mezzacapo, M. C.; Parente, A.; Landi, N.; Severino, V.; Di Maro, A. *Mol. Biotechnol.* **2014**, *56*, 738−746.

(8) Xianyu, Y.; Chen, Y.; Jiang, X. *Anal. Chem.* **2015**, *87*, 10688−10692.

(9) Grigorenko, V.; Andreeva, I.; Börchers, T.; Spener, F.; Egorov, A. *Anal. Chem.* **2001**, *73*, 1134−1139.

(10) Krainer, F. W.; Glieder, A. *Appl. Microbiol. Biotechnol.* **2015**, *99*, 1611−1625.

(11) Fu, J.; Liu, M.; Liu, Y.; Woodbury, N. W.; Yan, H. *J. Am. Chem. Soc.* **2012**, *134*, 5516−5519.

(12) Zhang, Y.; Lyu, F.; Ge, J.; Liu, Z. *Chem. Commun.* **2014**, *50*, 12919−12922.

(13) You, M.; Wang, R.; Zhang, X.; Chen, Y.; Wang, K.; Peng, L.; Tan, W. *ACS Nano* **2011**, *5*, 10090−10095.

(14) Gao, Y.; Roberts, C. C.; Zhu, J.; Lin, J. L.; Chang, C. E. A.; Wheeldon, I. *ACS Catal.* **2015**, *5*, 2149−2153.

(15) Childs, R. E.; Bardsley, W. G. *Biochem. J.* **1975**, *145*, 93−103.

(16) Matsuda, H.; Tanaka, H.; Blas, B. L.; Noseñas, J. S.; Tokawa, T.; Ohsawa, S. *Jpn. J. Exp. Med.* **1984**, *54*, 131−138.

(17) Tsujimura, S.; Tatsumi, H.; Ogawa, J.; Shimizu, S.; Kano, K.; Ikeda, T. *J. Electroanal. Chem.* **2001**, *496*, 69−75.

(18) Erel, O. *Clin. Biochem.* **2004**, *37*, 277−285.

(19) Zhang, Y.; Tsitkov, S.; Hess, H. *Nat. Catal.* **2018**, *1*, 276−281.

(20) Goral, V. N.; Ryabov, A. D. *IUBMB Life* **1998**, *45*, 61−71.

(21) Wolfenden, B. S.; Willson, R. L. *J. Chem. Soc., Perkin Trans. 2* **1982**, 805−812.

DOI: 10.1021/acs.analchem.9b04751
Anal. Chem. 2020, 92, 1502−1510

(22) Rodriguez-Lopez, J. N.; Hernández-Ruiz, J.; Garcia-Canovas, F.; Thorneley, R. N.; Acosta, M.; Arnao, M. B. *J. Biol. Chem.* **1997**, *272*, 5469−5472.
(23) Savenkova, M. I.; Newmyer, S. L.; Ortiz de Montellano, P. R. *J. Biol. Chem.* **1996**, *271*, 24598−24603.
(24) Campomanes, P.; Rothlisberger, U.; Alfonso-Prieto, M.; Rovira, C. *J. Am. Chem. Soc.* **2015**, *137*, 11170−11178.
(25) Hernández-Ruiz, J.; Arnao, M. B.; Hiner, A. N.; Garcia-Canovas, F.; Acosta, M. *Biochem. J.* **2001**, *354*, 107−114.
(26) Cleland, W. W. *Biochim. Biophys. Acta, Spec. Sect. Enzymol. Subj.* **1963**, *67*, 104−137.
(27) Fersht, A. R. *Enzyme Structure and Mechanism*, 2nd ed.; W. H. Freeman and Co.: New York, 1985.
(28) Chen, Q.; Liang, C.; Sun, X.; Chen, J.; Yang, Z.; Zhao, H.; Feng, L.; Liu, Z. *Proc. Natl. Acad. Sci. U. S. A.* **2017**, *114*, 5343−5348.
(29) Chen, J.; Zhou, X.; Yuan, T. *Synth. Commun.* **2014**, *44*, 3630−3636.
(30) Akiba, K.; Kawamura, T.; Ochiumi, M.; Inamoto, N. *Bull. Chem. Soc. Jpn.* **1976**, *49*, 1913−1916.
(31) Fei, J.; Basu, A.; Xue, F.; Palmore, G. T. *Org. Lett.* **2006**, *8*, 3−6.
(32) Gajhede, M.; Schuller, D. J.; Henriksen, A.; Smith, A. T.; Poulos, T. L. *Nat. Struct. Biol.* **1997**, *4*, 1032−1038.
(33) Ugarova, N. N.; Lebedeva, O. V.; Berezin, I. V. *J. Mol. Catal.* **1981**, *13*, 215−225.
(34) Zhang, Y.; Tsitkov, S.; Hess, H. *Nat. Commun.* **2016**, *7*, 13982.
(35) Rodríguez-López, J. N.; Lowe, D. J.; Hernández-Ruiz, J.; Hiner, A. N.; García-Cánovas, F.; Thorneley, R. N. *J. Am. Chem. Soc.* **2001**, *123*, 11838−11847.
(36) Zhao, Z.; Fu, J.; Dhakal, S.; Johnson-Buck, A.; Liu, M.; Zhang, T.; Woodbury, N. W.; Liu, Y.; Walter, N. G.; Yan, H. *Nat. Commun.* **2016**, *7*, 10619.
(37) Gao, Y.; Roberts, C. C.; Toop, A.; Chang, C. E.; Wheeldon, I. *ChemBioChem* **2016**, *17*, 1430−1436.
(38) Li, Z.; Zhang, Y.; Su, Y.; Ouyang, P.; Ge, J.; Liu, Z. *Chem. Commun.* **2014**, *50*, 12465−12468.
(39) Lu, S.; Hu, T.; Wang, S.; Sun, J.; Yang, X. *ACS Appl. Mater. Interfaces* **2017**, *9*, 167−175.
(40) Kamal, J. K.; Behere, D. V. *J. Inorg. Biochem.* **2003**, *94*, 236−242.
(41) Wilner, O. I.; Weizmann, Y.; Gill, R.; Lioubashevski, O.; Freeman, R.; Willner, I. *Nat. Nanotechnol.* **2009**, *4*, 249−254.
(42) Xin, L.; Zhou, C.; Yang, Z.; Liu, D. *Small* **2013**, *9*, 3088−3091.
(43) Idan, O.; Hess, H. *ACS Nano* **2013**, *7*, 8658−8665.
(44) Idan, O.; Hess, H. *Curr. Opin. Biotechnol.* **2013**, *24*, 606−611.
(45) Zhang, Y.; Hess, H. *ACS Catal.* **2017**, *7*, 6018−6027.
(46) Zhang, Y.; Wang, Q.; Hess, H. *ACS Catal.* **2017**, *7*, 2047−2051.
(47) Collins, J.; Zhang, T.; Oh, S. W.; Maloney, R.; Fu, J. L. *Chem. Commun.* **2017**, *53*, 13059−13062.
(48) Fu, Y.; Zeng, D.; Chao, J.; Jin, Y.; Zhang, Z.; Liu, H.; Li, D.; Ma, H.; Huang, Q.; Gothelf, K. V.; Fan, C. *J. Am. Chem. Soc.* **2013**, *135*, 696−702.
(49) Kadnikova, E. N.; Kostic, N. M. *J. Mol. Catal. B: Enzym.* **2002**, *18*, 39−48.
(50) Arnao, M. B.; Acosta, M.; Delrio, J. A.; Garciacanovas, F. *Biochim. Biophys. Acta, Protein Struct. Mol. Enzymol.* **1990**, *1038*, 85−89.
(51) Trinder, P. *J. Clin. Pathol.* **1969**, *22*, 158−161.
(52) Bateman, R. C.; Evans, J. A. *J. Chem. Educ.* **1995**, *72*, A240.
(53) Fornera, S.; Walde, P. *Anal. Biochem.* **2010**, *407*, 293−295.
(54) Voogd, C. E.; Van der Stel, J. J.; Jacobs, J. J. *J. Immunol. Methods* **1980**, *36*, 55−61.
(55) Moore, W. B.; Voogd, C. E. *Mutat. Res., Genet. Toxicol. Test.* **1983**, *118*, 43−47.
(56) Holland, V. R.; Saunders, B. C.; Rose, F. L.; Walpole, A. L. *Tetrahedron* **1974**, *30*, 3299−3302.
(57) Garner, R. C.; Walpole, A. L.; Rose, F. L. *Cancer Lett.* **1975**, *1*, 39−42.
(58) Xie, X.; Wang, C.; Xie, Y.; Wang, X.; Chen, G.; Yan, X. R.; Cui, J.; Chen, F.; Li, H.; Jin, B. *J. Immunol. Methods* **2013**, *396*, 65−73.
(59) Clotilde, L. M.; Bernard, C.; Salvador, A.; Lin, A.; Lauzon, C. R.; Muldoon, M.; Xu, Y.; Lindpaintner, K.; Carter, J. M. *J. Microbiol. Methods* **2013**, *92*, 226−230.
(60) Ueda, H.; Tsumoto, K.; Kubota, K.; Suzuki, E.; Nagamune, T.; Nishimura, H.; Schueler, P. A.; Winter, G.; Kumagai, I.; Mahoney, W. C. *Nat. Biotechnol.* **1996**, *14*, 1714−1718.
(61) Piletskaya, E. V.; Piletsky, S. A.; El'skaya, A. V.; Sozinov, A. A.; Marty, J. L.; Rouillon, R. *Anal. Chim. Acta* **1999**, *398*, 49−56.
(62) Liu, L.; Chen, F. C.; Dorsey, J. L.; Hsieh, Y. H. P. *J. Food Sci.* **2006**, *71*, M1.
(63) Carthew, P.; Gannon, J.; Whisson, I. *Lab. Anim.* **1981**, *15*, 69−73.
(64) Zhou, E. M.; Chan, M.; Heckert, R. A.; Riva, J.; Cantin, M. F. *Avian Dis.* **1998**, *42*, 517−522.
(65) Lee, H. Y.; Atlasevich, N.; Granzotto, C.; Schultz, J.; Loike, J.; Arslanoglu, J. *Anal. Methods* **2015**, *7*, 187−196.
(66) Piletsky, S. A.; Piletska, E. V.; Bossi, A.; Karim, K.; Lowe, P.; Turner, A. P. *Biosens. Bioelectron.* **2001**, *16*, 701−707.
(67) Mekaprateep, M.; Tharavichitkul, P.; Srikitjakarn, L. *J. Microbiol. Methods* **2010**, *83*, 266−269.
(68) Abuknesha, R. A.; Jeganathan, F.; Wu, J.; Baalawy, Z. *Nat. Protoc.* **2009**, *4*, 452−460.
(69) Hagen, E. C.; Andrassy, K.; Csernok, E.; Daha, M. R.; Gaskin, G.; Gross, W. L.; Hansen, B.; Heigl, Z.; Hermans, J.; Jayne, D.; Kallenberg, C. G. M.; Lesavre, P.; Lockwood, C. M.; Lüdemann, J.; Mascart-Lemone, F.; Mirapeix, E.; Pusey, C. D.; Rasmussen, N.; Sinico, R. A.; Tzioufas, A.; Wieslander, J.; Wiik, A.; Van der Woude, F. J. *J. Immunol. Methods* **1996**, *196*, 1−15.
(70) Uzal, F. A.; Carrasco, A. E.; Nielsen, K. H. *Vet. Res. Commun.* **1996**, *20*, 421−426.
(71) Lemos, M. A.; Oliveira, J. C.; Saraiva, J. A. *Lebensm. Wiss. Technol.* **2000**, *33*, 362−368.
(72) Chattopadhyay, K.; Mazumdar, S. *Biochemistry* **2000**, *39*, 263−270.

DOI: 10.1021/acs.analchem.9b04751
Anal. Chem. 2020, 92, 1502−1510